

# Constraining Cosmological Parameters through Double Source Plane Lensing

Jimena González

University of Wisconsin-Madison  
December 11, 2019

*Abstract:* Double Source Plane Lensing (DSPL) has been recently proposed as a complementary cosmological probe due to its sensitivity to the dark energy of equation parameters. For these systems, it is possible to define the variable  $\beta$  (ratio of distance ratios), whose sensitivity has been studied in [1] and it was found that it is very sensitive to the dark energy equation of state parameters. In particular, for low lens redshifts the contour ellipse on the  $\omega_0$  and  $\omega_a$  plane leans to the right, unlike the classical probes. In [2], two DSPL systems candidates of low redshift were identified and their properties were measured. In this project, we performed an statistical analysis of the data and we found that the information of these systems cannot be used to determine cosmological constraints because the uncertainties of the measurements are large and because the distribution of the redshifts of the systems is not optimal.

*Keywords:* Double source plane lensing, strong lensing, dark energy equation of state, cosmological constraints

## I. INTRODUCTION AND BACKGROUND

A DSPL is a system in which there is a foreground heavy galaxy (lens) with two sources on the background that are sufficiently align behind the lens that the light emitted by them gets bended by the gravitational potential of it. Thus, multiple images of the sources are created and the observer would recognized arcs of light produced by the sources. For a single lensing system the variable called Einstein radius can be defined as:

$$\theta_E^2 = \frac{4GM}{c^2} \frac{D_{LS}(z, z_1)}{D_L(z)D_S(z_1)} \quad (1)$$

Where  $M$  is the mass of the lens,  $z$  and  $z_1$  are the lens and source redshifts,  $D_{LS}(z, z_1)$ ,  $D_L(z)$  and  $D_S(z_1)$  are the angular diameter distances between the lens and the source, the lens and the observer and the source and the observer, respectively. For a DSPL system the variable  $\beta$  is defined as the ratio of the Einstein radius squared for each source, which is the ratio of distances ratio:

$$\beta = \frac{D_{LS}(z, z_1)}{D_S(z_1)} \frac{D_S(z_2)}{D_{LS}(z, z_2)} \quad (2)$$

Where  $z_2$  is the redshift of the second source (the furthest away from the lens). Since this variable is dimensionless, it is independent of the Hubble constant. In [1] it was studied the sensitivity of this variable to the cosmological parameters the dark energy equation of state today  $\omega_0$ , the dark energy equation of state time variation  $\omega_a$  and the matter density  $\Omega_m$ . Figure 1 shows the sensitivity of  $\beta$  to the redshift of the lens  $z$  through the Fisher derivatives  $\partial\beta/\partial p_i$  for the parameters  $\Omega_0$ ,  $\omega_a$  and  $\Omega_m$ .

The results are shown a flat  $\Lambda$ CDM universe cosmology with  $\Omega_m = 0.3$  and for redshifts of the sources that satisfy:  $z_1 = 2z$  and  $z_2 = 1.5z$ . The larger the absolute magnitude of the sensitivity and the greatest the distinction between the curves, the more information can be extracted from the figures and the tighter are the constraints on the cosmological parameters.

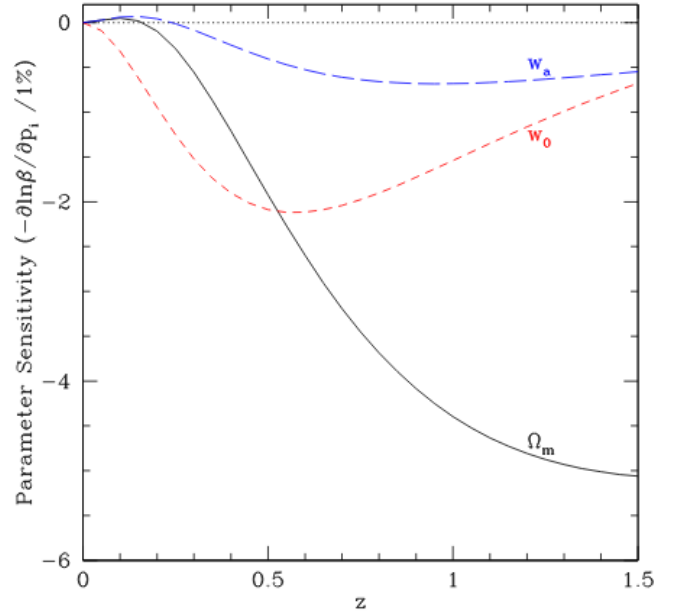


FIG. 1. Plot of the parameter sensitivity: Negative derivative of  $\ln \beta$  with respect to each cosmological parameter  $\omega_0$ ,  $\omega_a$  and  $\Omega_m$  vs redshift of the lens. In this figure it was assumed a redshift distribution of:  $z_1 = 2z$  and  $z_2 = 1.5z$ . Image taken from [1].

For a lens redshift of around 0.15 the sensitivity is in-

dependent of  $\Omega_m$ , for redshifts lower than 0.23,  $\Omega_0$  and  $\Omega_a$  are positive correlated and the sensitivity is greater for  $\Omega_0$  and  $\Omega_a$  than  $\Omega_m$ . While for classical cosmological probes  $\omega_0$  and  $\omega_a$  have a negative correlation and  $\beta$  is more sensitive to the matter density. Figure 2 shows the constraints estimated in [1] for the cosmological parameters. The solid ellipses represent the constraints on the cosmological parameters by fixing  $\Omega_m = 0.3$ . When the lens redshift is 0.23 the contour figure is vertical and for lower redshifts the ellipse leans to the right, unlike for classical probes. For this reason, DSPL is a potential complementary probe to constraint cosmological parameters.

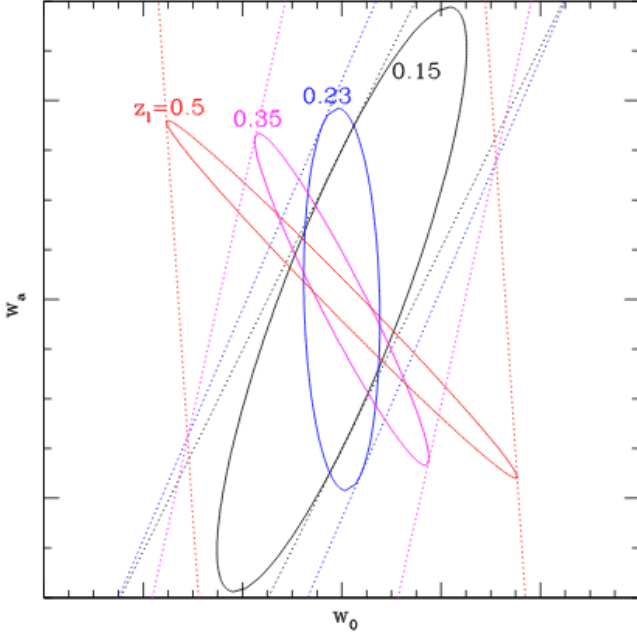


FIG. 2. Plot estimating the constraints on the dark energy equation of state parameters for different lens redshifts  $z$ . Image taken from [1].

Last year (2018) two DSPL systems candidates were identified in the Sloan Digital Sky Survey (SDSS) data [2]. The systems identified are the following:

- Plate-IFU: 8131-6102. Redshifts:  $z=0.04956$ ,  $z_1=0.694$  and  $z_2=0.954$ . Einstein radii:  $\theta_1 = 2.74^{+0.13}_{-1.56}$  and  $\theta_2 = 2.77^{+0.19}_{-1.57}$ . System shown in panels (1a) and (1b) in Figure 3.
- Plate IFU: 8947-6104. Redshifts:  $z=0.04865$ ,  $z_1=0.165$  and  $z_2=0.264$ . Einstein radii:  $\theta_1 = 1.85^{+0.06}_{-1.13}$  and  $\theta_2 = 2.27^{+0.08}_{-1.50}$ . System shown in panels (2a) and (2b) in Figure 3.

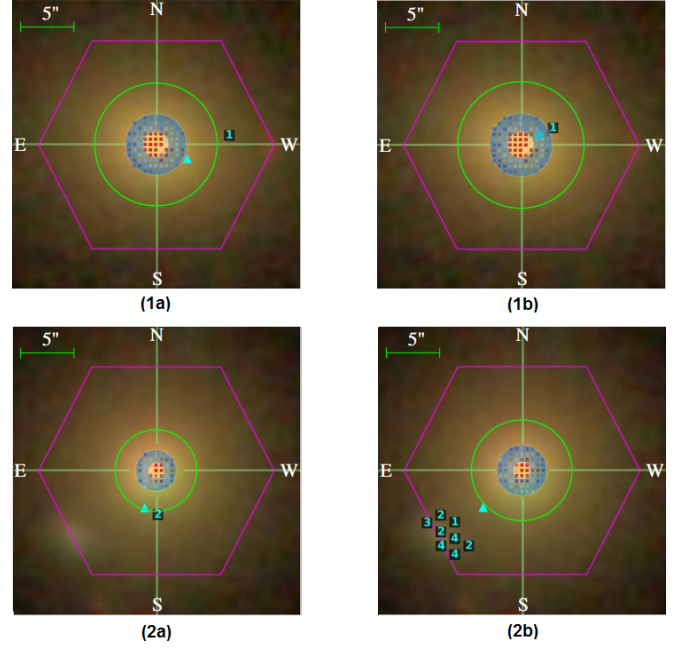


FIG. 3. Plots of sources emission line hits. The cyan numbers represent the position of the hits. The inner and outer radii of the cyan circle represent the lower and upper limit of the Einstein radius. Image taken from [2].

Furthermore, [2] provides additional information about the systems like their SDSS System Name, their NSA Sersic effective radius, the number of good background emission-line hits identified within the common source-plane and the ratio of the radial distance of a source-plane image's detectable edge to the upper limit of the Einstein radius.

Both lenses of these systems have a redshift lower than 0.23. Thus, it is expected that by performing a statistical analysis of available information we could set constraints on the dark energy equation of state parameters.

## II. THEORY AND METHODOLOGY

In order to perform the statistical analysis on the data we need to know how to calculate the Einstein radius for a system with known redshifts and arbitrary values for  $\omega_0$  and  $\omega_a$ . First, let's start with the definition of comoving distance:

$$d_c = \frac{c}{H_0} \int_0^z \frac{1}{E(z')} dz' = d_h \int_0^z \frac{1}{E(z')} dz' \quad (3)$$

$E(z)$  is defined as:

$$E(z) \equiv \frac{H(z)}{H_0} = \sqrt{\Omega_{rad} a^{-4} + \Omega_m a^{-3} + \Omega_k a^{-2} + \Omega_{DE} a^{-3(1+w)}} \quad (4)$$

Where  $H_0$  is the Hubble constant,  $z$  the redshift of the object and  $a$  is the scale factor  $a = 1/(1+z)$ . For a curved universe the comoving distance is generalized to the expression:

$$d_M = \begin{cases} \frac{d_H}{\sqrt{\Omega_K}} \sinh\left(\frac{\sqrt{\Omega_K} d_c}{d_H}\right) & \Omega_K > 0 \\ d_c & \Omega_K = 0 \\ \frac{d_H}{\sqrt{\Omega_K}} \sin\left(\frac{\sqrt{\Omega_K} d_c}{d_H}\right) & \Omega_K < 0 \end{cases}$$

Finally, the angular diameter distance is defined as:

$$D = \frac{d_M}{1+z} \quad (5)$$

Assuming the cosmology of a flat universe ( $\Omega_K=0$ ) and matter and a dark energy dominated universe ( $\Omega_{rad}=0$ ), we obtain  $d_M = d_c$ . In addition, we must choose a parametrization for  $\omega(a)$  the dark energy equation of state. We first consider the non-constant parametrization introduced by Chevallier-Polarsky-Linder [3],[4], given by:

$$\omega(a) = \omega_0 + \omega_a \frac{z}{z+1} \quad (6)$$

Thus, in our case of study the angular diameter distance and the variable  $E(z)$  would be given by equations 7 and 8, respectively. Hence, by picking specific values for  $\omega_0$  and  $\omega_a$ , we can use these expressions to find the angular diameter distance of an object with known redshift. Then, we can calculate the variable  $\beta$  of a DSPL system by taking the ratio of the angular diameter distance ratio for each source with the lens.

$$D = \frac{d_h}{1+z} \int_0^z \frac{1}{E(z')} dz' \quad (7)$$

$$E(z) = \sqrt{\Omega_m a^{-3} + \Omega_{DE} a^{-3(1+\omega_0+\omega_a)} e^{-3\omega_a(1-a)}} \quad (8)$$

The objective of this project is to find the values of  $\omega_0$  and  $\omega_a$  that produce the closest value to the  $\beta$  measured by [2] using the equations above given the value of the lens and sources redshifts. The first approach would be performing a reduced chi-squared statistic analysis on the data, which is a method used extensively in goodness of fit testing. The chi square function can be written as:

$$\chi^2 = \sum_i \frac{(y_i - \tilde{y}_i)^2}{\sigma_i^2} \quad (9)$$

Where  $y_i$  are the observed data values,  $\tilde{y}_i$  are the predicted values from the theory (expected values) and  $\sigma_i$  are the uncertainties of the individual experimental values. By minimizing the chi square function it is possible to find the optimal values of the parameters in the theoretical model. In our study, we know the value of  $\beta$  and its uncertainty for two candidate DSPL systems, and we know how the theoretical model for  $\beta$  depends on the  $\omega_0$  and  $\omega_a$  parameters given certain values of redshift. Thus, by varying each of these parameters we can minimize the chi square function and find the optimal values of  $\omega_0$  and  $\omega_a$  that reproduce the best the experimental data. In order to increase the efficiency of this method it is possible to perform the Metropolis-Hastings algorithm to find the optimal values of the parameters faster. Finally, we could represent in a graph of  $\omega_0$  vs  $\omega_a$  contours representing the values of these parameters that reproduce the better the experimental data and from these determine constraints on the dark energy equation of state parameters.

### III. ANALYSIS & RESULTS

We can calculate the value of the  $\beta$  variable and its uncertainty for each system by taking the ratio of the Einstein radii squared and taking into account its propagation of uncertainty. Since the upper and lower limit of the uncertainty related to each measurement of the Einstein radius is different, our first approach is to take the average of both limits and calculate the uncertainty of  $\beta$  using the variance formula (equation 10).

$$\sigma_\beta = \sqrt{\left(\frac{\partial \beta}{\partial \theta_1}\right)^2 \theta_1^2 + \left(\frac{\partial \beta}{\partial \theta_2}\right)^2 \theta_2^2} \quad (10)$$

For the first system with lens redshift of 0.04956 we found the "experimental"  $\beta_1$  to be  $0.978456646 \pm 0.866436694$  and for the second systems with lens redshift of 0.04865 we calculated  $\beta_2 = 0.664189097 \pm 0.629484119$ . The uncertainty related to each experimental value is very high, so it is expected that the cosmological constraints that will be set on this project won't be very tight. This occurs because even though the upper limits of the Einstein radii for each system are low, the lower limits are very high compare to the measured value.

As it was mentioned before, we assumed a flat universe ( $\Omega_K=0$ ) and matter and a dark energy dominated universe ( $\Omega_{rad}=0$ ), we used a value of 0.23 as the matter density today ( $\Omega_m$ ), and a value of 0.73 for the dark energy density today. In addition, we used the non-constant parametrization of the dark energy equation of state given by equation 6.

To calculate the integral in the expression for the angular diameter distance (7) we use the the python SciPy function called quad which uses a technique from the Fortran

library QUADPACK. The error associated to this function for calculating angular diameter distances is about 17 orders of magnitude lower than the value determined for chosen values of  $\omega_0$  and  $\omega_a$ .

To perform the reduced chi-squared analysis of the data, we calculated the "theoretical" value of  $\beta$  given the values of the redshift of the objects in the system, using equation 7 and 2 for certain values of  $\omega_0$  and  $\omega_a$ . Then, to calculate the chi square function (equation 9) we only need to sum two terms since we only have two experimental values measured.

In [5] Li and Xia studied observational data to determine the dark energy equation of state parameters. From their results we can expect that  $\omega_0$  will be in the range from -1.5 to -0.5 and  $\omega_a$  will be in the range from -2.5 to 1.5. The results for this project are shown in Figure 4, which shows the value of  $\chi^2$  as a color map that was calculated for a different values of  $\omega_0$  and  $\omega_a$  in the expected range of these parameters. In this graph we can see that for the selected ranges of the parameters, the value  $\chi^2$  is minimum for large values of  $\omega_0$  and small values of  $\omega_a$ . However, we cannot extract much information of the figure since it does not display the expected behaviour of contour ellipses as in in [5] and in Figure 2. Moreover, the values of  $\chi^2$  are very low, which indicates that this model is "too good" to fit the data and this is coherent with the large uncertainties of the measurements. It is also important to mention that in [1] was determined that the greatest sensitivity would be obtain for a system in which the ratios  $z/z_1$  and  $z_2/z_1$  are close to unity and a large value compare to unity, respectively. Regardless, for the first system the ratios are  $z/z_1 = 14.00$  and  $z_2/z_1 = 1.374$ , and for the second system they are  $z/z_1 = 3.392$  and  $z_2/z_1 = 1.6$ . These distributions of redshifts explain the shape of the plot.

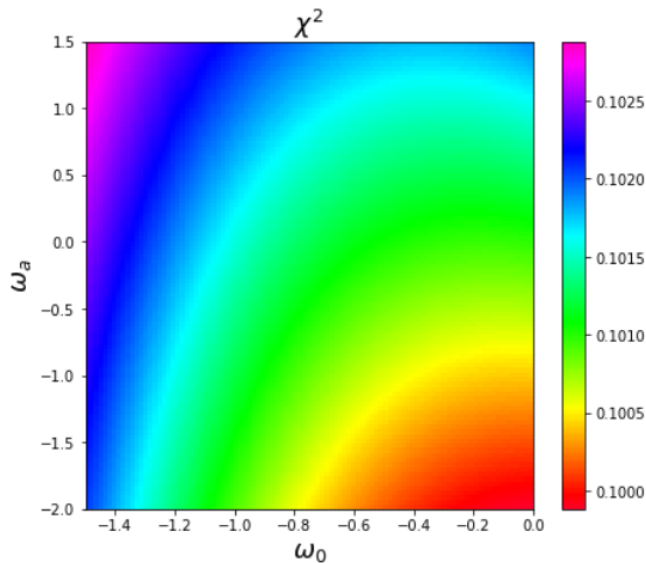


FIG. 4. Contour plot in the  $w_0$  and  $w_a$  plane representing the value  $\chi^2$  as a colormap for different values of  $\omega_0$  and  $\omega_a$ .

For the rest of the project, we wanted to study how the contour plots would change by reducing the uncertainties of the data, using higher quality data, and changing the distribution of the redshifts.

Figure 5 shows the contour plots we would get if we only use the upper limits of the uncertainties for the Einstein radii. In this case, the measured betas would be:  $\beta_1 = 0.97846 \pm 0.16321$  and  $\beta_2 = 0.66419 \pm 0.06362$ . The uncertainties of these measurements are much lower than before so the values of  $\chi^2$  increase, but the shape of the figure does not change significantly.

Figure 6 shows the contour plots we would get by using values of the Einstein radii that are closer to the predicted value for a cosmology of  $w_0 = -1$  and  $w_a = 0$  and by reducing the Einstein radii uncertainties. The measured betas are  $\beta_1 = 0.97023 \pm 0.02765$  and  $\beta_2 = 0.87048 \pm 0.02552$ . While the predicted betas for the chosen cosmology were  $\beta_1 = 0.98014$  and  $\beta_2 = 0.86480$ . This plot shows an improved behaviour of the contour curves that look more like an ellipse that is leaning to the left. However, the uncertainties in the measurements needed to obtain this behaviour must be very low.

Figure 7 shows the contour plots we would get by using the most effective redshift distribution given by  $z_1 = 2z$  and  $z_2 = 1.5z$ , where  $z$  is the redshift of the lens for each system. Also, we used values of the measured Einstein radii that close to the predicted value in a cosmology of  $w_0 = -1$  and  $w_a = 0$ . For this case, the measured betas were  $\beta_1 = 0.74649 \pm 0.22836$  and  $\beta_2 = 0.75342 \pm 0.22988$ . This plot exhibit a noticeable improvement of the contours, and it possible to see that there is a region inside the range of  $w_0$  and  $w_a$  for which the  $\chi^2$  is minimal. In Figure 8 the only difference was that we used values of the measured Einstein radii that were very close to the predicted value in the chosen cosmology. For this case, the measured betas were  $\beta_1 = 0.75013 \pm 0.22916$  and  $\beta_2 = 0.75013 \pm 0.22916$ . This figure shows an improvement in the contour curves and the region in which  $\chi^2$  is reduced, which would represent tighter cosmological constraints.

Figure 9 shows the contour plots we would get by using higher values of the lens's redshifts for both systems (0.5 and 0.6), the most effective redshift distribution  $z_1 = 2z$  and  $z_2 = 1.5z$ , and values of the measured Einstein radii that are close to the predicted value in a cosmology of  $w_0 = -1$  and  $w_a = 0$ . In this case, the measured betas were  $\beta_1 = 0.75568 \pm 0.23037$  and  $\beta_2 = 0.75603 \pm 0.23044$ . This plot shows better contour curves, that could set tighter cosmological constraints. This is expected, since in figure 2 the sensitivity is the greatest for a lens's redshift close to 0.5. However, the ellipse leans to the left, which is the same behaviour that is observed from classical cosmological probes, so these systems would not provide much additional information.

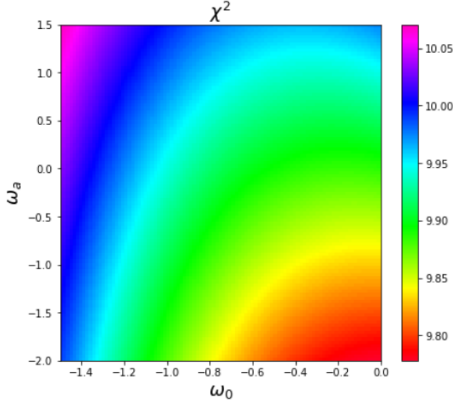


FIG. 5. Contour plot in the  $w_0$  and  $w_a$  plane obtained by using only the upper limits of the Einstein radii uncertainty. Measured betas:  $\beta_1 = 0.97846 \pm 0.16321$  and  $\beta_2 = 0.66419 \pm 0.06362$ .

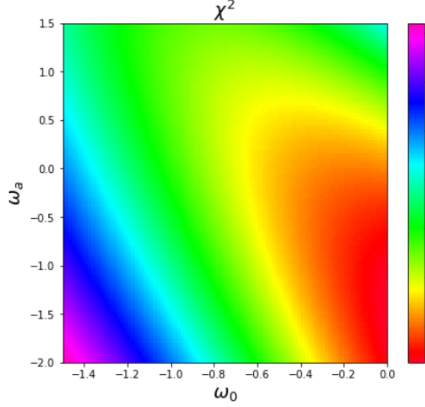


FIG. 6. Contour plot in the  $w_0$  and  $w_a$  plane obtained by using reducing the uncertainty in the Einstein radii and using values of the measured Einstein radii that are closer to the predicted value using a cosmology of  $w_0 = -1$  and  $w_a = 0$ . Measured betas:  $\beta_1 = 0.97023 \pm 0.02765$  and  $\beta_2 = 0.87048 \pm 0.02552$ .

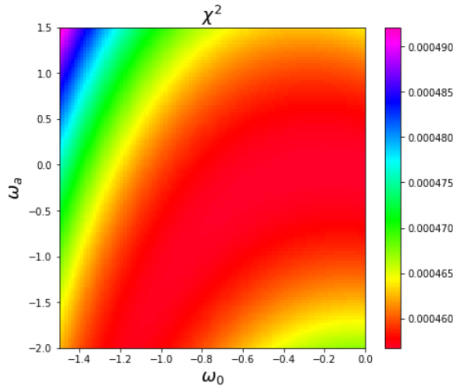


FIG. 7. Contour plot in the  $w_0$  and  $w_a$  plane obtained by using the most effective redshift distribution  $z_1 = 2z$  and  $z_2 = 1.5z$ , and values of the measured Einstein radii that are closer to the predicted value in a cosmology of  $w_0 = -1$  and  $w_a = 0$ . Measured betas:  $\beta_1 = 0.74649 \pm 0.22836$  and  $\beta_2 = 0.75342 \pm 0.22988$ .

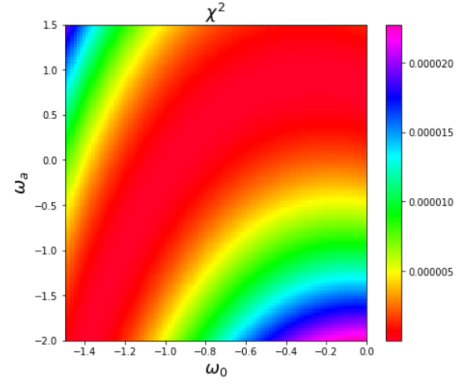


FIG. 8. Contour plot in the  $w_0$  and  $w_a$  plane obtained by using the most effective redshift distribution  $z_1 = 2z$  and  $z_2 = 1.5z$ , and values of the measured Einstein radii that are almost the predicted value in a cosmology of  $w_0 = -1$  and  $w_a = 0$ . Measured betas:  $\beta_1 = 0.75013 \pm 0.22916$  and  $\beta_2 = 0.75013 \pm 0.22916$ .

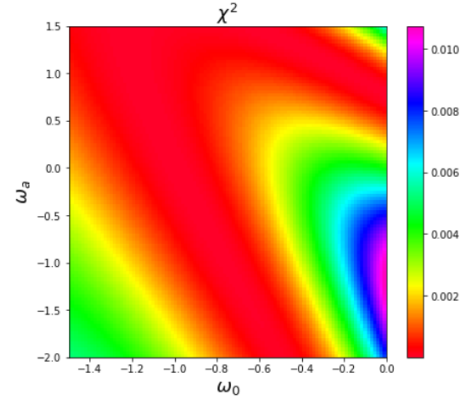


FIG. 9. Higher effective redshift distribution and predicted Einstein radii Contour plot in the  $w_0$  and  $w_a$  plane obtained by using a high effective redshift distribution  $z_1 = 2z$  and  $z_2 = 1.5z$  (with  $z=0.5$  and  $z=0.6$ , for each system), and values of the measured Einstein radii that are close to the predicted value in a cosmology of  $w_0 = -1$  and  $w_a = 0$ . Measured betas:  $\beta_1 = 0.75568 \pm 0.23037$  and  $\beta_2 = 0.75603 \pm 0.23044$ .

#### IV. CONCLUSIONS

The  $\chi^2$  plot for both of the found systems does not provide much information to constraint cosmological parameters. This is because the uncertainties of the Einstein radii are too large, but also the systems do not have an optimal distribution of redshifts. By using only the smallest uncertainties of the Einstein radii the plot does not change significantly. However, by using a measurement of higher quality (measured values closer to the predicted values and lower uncertainties) the behaviour of the plot changes and the figure displays a more ellipsoidal shape. We observed that by changing the distribution of the redshift the  $\chi^2$  plot changes significantly. Thus, we

conclude that it more important for setting constraint on dark energy cosmological parameters to have systems with a redshift distribution similar to the most effective distribution:  $z_1 = 2z$  and  $z_2 = 1.5z_1$  than to have low uncertainties in the measurements. As it was stated before,

this analysis would be more sensitive to higher values of  $z_2/z_1$ , but in this project we didn't include higher values for this ratio since it would be harder to obtain precise measurements for this case, as the uncertainties in beta must be very low.

- 
- [1] Eric V. Linder. Doubling strong lensing as a cosmological probe. *Phys. Rev. D*, 94:083510, Oct 2016.
  - [2] *Monthly Notices of the Royal Astronomical Society*, 2018.
  - [3] Eric V. Linder. Exploring the expansion history of the universe. *Physical Review Letters*, 90(9), Mar 2003.
  - [4] MICHEL CHEVALLIER and DAVID POLARSKI. Accelerating universes with scaling dark matter. *International Journal of Modern Physics D*, 10(02):213–223, Apr 2001.
  - [5] Hong Li and Jun-Qing Xia. Constraints on dark energy parameters from correlations of cmb with lss. *Journal of Cosmology and Astroparticle Physics*, 2010(04):026–026, Apr 2010.